



A Review Study on Sulfate-Radical-Based Advanced Oxidation Processes for Domestic/Industrial Wastewater Treatment: Degradation, Efficiency, and Mechanism

Xinhui Xia¹, Fengyi Zhu¹, Jianju Li¹, Haizhou Yang¹, Liangliang Wei^{1*}, Qiaoyang Li¹, Junqiu Jiang¹, Guangshan Zhang² and Qingliang Zhao¹

¹ State Key Laboratory of Urban Water Resources and Environment (SKLUWRE), School of Environment, Harbin Institute of Technology, Harbin, China, ² College of Resource and Environment, Qingdao Agricultural University, Qingdao, China

OPEN ACCESS

Edited by:

Marc Pera-Titus,
Fudan University, China

Reviewed by:

Nito Angelo Debacher,
Federal University of
Santa Catarina, Brazil
Taner Yonar,
Uludağ University, Turkey

*Correspondence:

Liangliang Wei
weill333@163.com

Specialty section:

This article was submitted to
Green and Sustainable Chemistry,
a section of the journal
Frontiers in Chemistry

Received: 06 August 2020

Accepted: 21 October 2020

Published: 27 November 2020

Citation:

Xia X, Zhu F, Li J, Yang H, Wei L, Li Q,
Jiang J, Zhang G and Zhao Q (2020)
A Review Study on
Sulfate-Radical-Based Advanced
Oxidation Processes for
Domestic/Industrial Wastewater
Treatment: Degradation, Efficiency,
and Mechanism.
Front. Chem. 8:592056.
doi: 10.3389/fchem.2020.592056

High levels of toxic organic pollutants commonly detected during domestic/industrial wastewater treatment have been attracting research attention globally because they seriously threaten human health. Sulfate-radical-based advanced oxidation processes (SR-AOPs) have been successfully used in wastewater treatment, such as that containing antibiotics, pesticides, and persistent organic pollutants, for refractory contaminant degradation. This review summarizes activation methods, including physical, chemical, and other coupling approaches, for efficient generation of sulfate radicals and evaluates their applications and economic feasibility. The degradation behavior as well as the efficiency of the generated sulfate radicals of typical domestic and industrial wastewater treatment is investigated. The categories and characteristics of the intermediates are also evaluated. The role of sulfate radicals, their kinetic characteristics, and possible mechanisms for organic elimination are assessed. In the last section, current difficulties and future perspectives of SR-AOPs for wastewater treatment are summarized.

Keywords: sulfate-radicals, wastewater, activation approaches, degradation kinetics, reaction mechanisms

INTRODUCTION

The ongoing development of industries and agriculture has resulted in increasing discharge of toxic organic contaminants such as pesticides, antibiotics, dyes, and pharmaceuticals into drainage systems and, consequently, into wastewater treatment plants (WWTPs). These toxic organic pollutants have attracted considerable attention recently (Martin-Diaz et al., 2020; Qin et al., 2020b; Seleiman et al., 2020). Owing to the high toxicity, polymeric structures, and non-biodegradable characteristics of these pollutants, traditional biological treatment approaches for WWTPs are not effective as they cannot destroy their structures. The treatment works thus fail to address the ultimate eradication of these substances (Babu et al., 2019). In addition, some of the widely used physical (e.g., filtration, flotation) or chemical (e.g., chemical coagulation and electrochemistry) processes have also been criticized for the high production of solid waste and secondary contamination. There is therefore a need to explore alternatives for effective and

environmentally friendly treatment of these organic contaminants, to provide a better approach for degradation of these hazardous wastes before effluent is discharged into aquatic environments.

Advanced oxidation processes (AOPs) are characterized by being easy to implement, highly efficient, environmentally compatible, and capable of oxidizing a wide range of contaminants (mineralization to CO_2 , H_2O , and inorganic ions). Further, they have been widely applied in refractory contaminant degradation (Huang and Zhang, 2019). Specifically, the generated free radicals, such as hydroxyl radical ($\text{OH}\cdot$), superoxide radicals ($\text{O}_2^{\cdot-}$), and sulfate radicals ($\text{SO}_4^{\cdot-}$), and hole (h^+) play a significant role in pollutant degradation. However, the application of $\text{OH}\cdot$ -based AOPs is partially limited because of the necessary acidic environmental conditions (pH 2–4) and H_2O_2 instability (Liu et al., 2018b).

Among the AOPs mentioned above, activated persulfate (PS) oxidation has been widely studied recently for a relatively long lifetime (30–40 μs) of the sulfate radicals ($\text{SO}_4^{\cdot-}$, $E_0 = 2.5\text{--}3.1\text{ V}$) and under moderate reaction conditions (4 < pH < 9) (Ren et al., 2015). In overall, sulfate radical advanced oxidation processes (SR-AOPs) have the following advantages: (i) higher redox potential of $\text{SO}_4^{\cdot-}$ ($E_0 = 2.5\text{--}3.1\text{ V}$ vs. NHE) than that of $\text{OH}\cdot$ ($E_0 = 1.8\text{--}2.7\text{ V}$ vs. NHE); (ii) more moderate reactional pH conditions of 2.0–8.0; (iii) longer half-life ($t_{1/2} = 30\text{--}40\ \mu\text{s}$) (Li et al., 2019a); and (iv) higher oxidation capacity in both carbonate and phosphate buffer solutions (Li et al., 2016; Liu et al., 2018b; Yang Q. et al., 2019). Hence, SR-AOPs are regarded as the most promising advanced oxidation processes for water and wastewater treatments.

Generally, peroxydisulfate (PDS) or PS can be activated to generate $\text{SO}_4^{\cdot-}$ radicals via appropriate heating, ultraviolet (UV) irradiation, or transition metal (Fe^{2+} , Co^{2+} , Ag^+) activation (Cai et al., 2015; Li et al., 2015; Yang W. et al., 2019). For example, sulfate radicals can be spontaneously produced from PS or PMS via the physical activation methods: (1) heating (Ji et al., 2016b), (2) light radiation (Khan et al., 2017), (3) ultrasonic waves (Deng et al., 2015), and the chemical activation approaches: (4) transition metal ion activation (Chen et al., 2019), (5) alkaline activation (Fernandes et al., 2018), (6) strong oxidizers (M'Arimi et al., 2020), and (7) electrochemistry activation (Li et al., 2019a). Innovative research of SR-AOPs mainly includes (1) new catalytic activation approaches, (2) novel role of free radicals, and (3) new degradation pathways and mechanisms. To further clarify the potential mechanisms of the activation, oxidation, and elimination processes of sulfate radicals, the relevant findings are summarized here.

In this paper, we first summarize the activation methods of PMS and PS for efficient sulfate radical generation. The efficiency of the various activation methods on PS and PMS is then evaluated via feasibility, key parameters, and economic analysis. Third, the possible mechanisms for degradation of organic pollutants using sulfate radicals are described. Finally, the challenges and perspectives for sulfate-radical-based advanced oxidation processes are put forward.

SULFATE RADICAL GENERATION AND EFFICIENCY IMPROVEMENT

Properties of PMS and PS

Sulfate radicals can be efficiently generated via the activation of PSs, such as peroxydisulfate (PDS, $\text{S}_2\text{O}_8^{2-}$) and permonosulfate (PMS, HSO_5^-) (Waclawek et al., 2017; Yang W. et al., 2019), both of which are characterized by the presence of an O–O bond (similar to hydrogen peroxide). Generally, PMS, a typical compound salt, mainly consists of potassium hydrogen sulfate, potassium sulfate, and potassium peroxydisulfate at a ratio of 1:1:2 (Waclawek et al., 2017). In contrast, PDS contains sulfate ions and positive ions.

The asymmetric structure of PMS, generated via the substitution of hydrogen atoms in H_2O_2 by SO_3 , is characterized by an O–O bond distance of 1.453 Å (Li et al., 2016). In comparison, PDS possesses a longer bond distance (1.497 Å) and lower bond energy (33.5 kcal mol⁻¹), which is closely related to the substitution of two individual hydrogen atoms of H_2O_2 by SO_3 (Xiao et al., 2018; Song et al., 2019). Thus, theoretically, the chemical characteristics for PDS are more stable than for PMS; PDS also has a higher redox potential than PMS (2.01 vs. 1.77 V) (Waclawek et al., 2017; Xiao et al., 2020). Overall, both PDS and PMS have been widely applied, owing to their excellent water solubility, low cost, ease of storage, and low environmental impact (Xiao et al., 2020). Traditionally, PS refers to PDS, including $\text{Na}_2\text{S}_2\text{O}_8$, $\text{K}_2\text{S}_2\text{O}_8$, and $(\text{NH}_4)_2\text{S}_2\text{O}_8$ (Tsitonaki et al., 2010; Li et al., 2019b). Among them, $\text{Na}_2\text{S}_2\text{O}_8$ has been frequently applied because of its lower cost, stable chemical characteristics, and ease of solubility.

Activation Approaches

The activation of PS and PMS is mainly conducted through thermal treatment, UV radiation, use of alkaline, and metal ion reactions. There is a wide variation between sulfate radicals produced by different activation approaches of the PS and PMS, in terms of activation mechanisms, pathways, and redox potential (see Table 1). Thus, summarizing the efficiency of different approaches of PS and PMS is fundamental to listing the critical targets of generation of sulfate radicals (see Figure 1).

Physical Activation Approaches

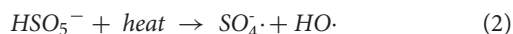
Thermal Activation

Thermolysis has traditionally been recognized as one of the most effective approaches for activating PS/PMS for $\text{SO}_4^{\cdot-}$ generation (Equations 1 and 2) (Zhou et al., 2019), despite intensive energy demand. The recent work of Ji et al. (2016b) showed that the ambient temperature ($20 \pm 1^\circ\text{C}$) could not activate PS efficiently for the purpose of tetracycline (TTC) oxidization, whereas there was complete elimination of TTC at 70°C after 30 min reaction under acidic conditions. This clearly demonstrated that high temperature promotes the formation of sulfate radicals. A similar result was also obtained by Zhou et al. (2019), who observed a significant enhancement of PS decomposition and $\text{SO}_4^{\cdot-}$ generation as the temperature increased from 20 to 75°C . Simultaneously, a noteworthy increase in acidic by-product formation was also observed (Zhou et al., 2019). For soil samples,

TABLE 1 | Summary of the different persulfate (PS) and peroxymonosulfate (PMS) activation approaches: pathways, mechanism, and key parameters.

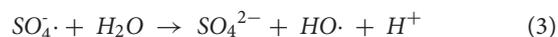
Activation approaches		Main reaction for sulfate radicals production	Mechanism	Key parameters	References
Physical activation	Heating	$S_2O_8^{2-} + heat \rightarrow 2SO_4^{\cdot-}$ (PS) $H_2SO_5 + heat \rightarrow SO_4^{\cdot-} + HO\cdot$ (PMS)	Fission of O–O bond	(i) Higher temperature can cleave O–O bond, whereas excessive temperature may cause side effects (ii) Owing to huge energy demand, not suitable for large-scale sewage treatment	Zhao et al., 2013; Wang and Wang, 2018
	UV	$S_2O_8^{2-} + h\nu \rightarrow 2SO_4^{\cdot-}$ (PS) $H_2SO_5 + h\nu \rightarrow SO_4^{\cdot-} + HO\cdot$ (PMS)	Fission of O–O bond	Usually under 254 nm wavelength, depending on dissolved oxygen concentration	Yang Q. et al., 2019
	Ultrasound	$S_2O_8^{2-} + 2H_2O \xrightarrow{OH^{\cdot}} HO_2^{\cdot} + 2SO_4^{2-} + 3H^+$ $S_2O_8^{2-} + 2HO_2^{\cdot} \rightarrow SO_4^{\cdot-} + SO_4^{2-} + H^+ + O_2^{\cdot-}$ (PS)	Fission of O–O bond Hydrolysis of water molecules	Similar to heating activation	Nasseri et al., 2017
Chemical activation	Alkaline activation	$S_2O_8^{2-} + H_2O \rightarrow HO_2^{\cdot} + 2SO_4^{2-} + H^+$ $S_2O_8^{2-} + HO_2^{\cdot} \rightarrow SO_4^{\cdot-} + SO_4^{2-} + H^+ + O_2^{\cdot-}$ (PS) $H_2SO_5 \rightarrow SO_5^{\cdot-} + H^+$ $H_2SO_5 + H_2O \rightarrow HSO_4^{\cdot} + H_2O_2$ $SO_5^{\cdot-} + H_2O \rightarrow SO_4^{2-} + H_2O_2$ $H_2O_2 \rightarrow HO_2^{\cdot} + H^+$ $H_2O_2 \rightarrow 2OH\cdot$ $H_2O_2 + OH\cdot \rightarrow HO_2^{\cdot} + H_2O$ $HO_2^{\cdot} \rightarrow H^+ + O_2^{\cdot-}$ $HO\cdot + O_2^{\cdot-} \rightarrow {}^1O_2 + OH^-$ $2H^+ + 2O_2^{\cdot-} \rightarrow {}^1O_2 + H_2O_2$ $H_2SO_5 + SO_5^{\cdot-} \rightarrow HSO_4^{\cdot} + SO_4^{\cdot-} + {}^1O_2$ (PMS)	Hydrolysis of PS and PMS to hydrogen peroxide	Often pH > 11 For PMS activation, 1O_2 is the predominant radical specie, whereas $SO_4^{\cdot-}/OH\cdot/{}^1O_2$ for PS	Fernandes et al., 2018
	Transition metal ions	$S_2O_8^{2-} + M^{n+} \rightarrow M^{n+1} + SO_4^{2-} + SO_4^{\cdot-}$ (PS) $H_2SO_5 + M^{n+} \rightarrow M^{n+1} + OH^{\cdot} + SO_4^{\cdot-}$ (PMS)	Single electron transfer	Preparation of catalysts is more economical for a homogeneous system than that of a heterogeneous system	Liu L. et al., 2019
	Carbon-based materials	$S_2O_8^{2-} + AC_{surface} - OOH \rightarrow SO_4^{\cdot-} + AC_{surface} - OO\cdot + HSO_4^-$ $S_2O_8^{2-} + AC_{surface} - OH \rightarrow SO_4^{\cdot-} + AC_{surface} - O\cdot + HSO_4^-$ (PS) $H_2SO_5 + C - \pi \rightarrow C - \pi^{\cdot+} + SO_4^{\cdot-} + OH^-$ $H_2SO_5 + C - \pi^{\cdot+} \rightarrow C - \pi + SO_5^{\cdot-} + H^+$ (PMS)	Single electron transfer	Activated carbon is relatively economical	Zhao et al., 2017

Deng et al. (2015) found that increased temperature promoted PS oxidization of phenanthrene. However, Tsitonaki et al. (2010) found that high temperatures can negatively affect the transport of PS into soil; they can further affect the overall removal behavior of organics in soil (Zhao et al., 2013). Overall, thermal activation is not applicable to PS/PMS activation for large-scale soil remediation (Wang and Wang, 2018).



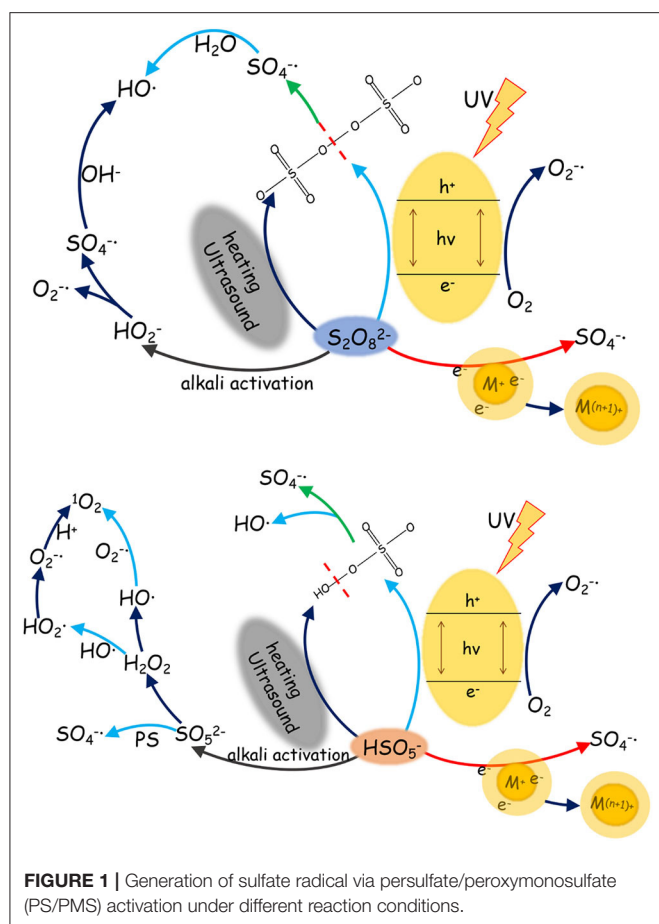
Fission of the O–O bond of PS/PMS at temperatures > 50°C (energy input 140.0–213.3 kJ/mol) during heating activation plays an essential role in the formation of sulfate radicals (Wang and Wang, 2018). Meanwhile, the generated sulfate radicals would quickly be converted to hydroxyl radicals and would subsequently cause a decrease in pH of the aqueous solution (Yang et al., 2010) (Equation 3). In addition, Yang et al. (2010) reported that the degradation efficiency of the

heat-activated PS was higher than that of PMS, which may be attributed to the higher O–O bond energy of PMS than that of PS.

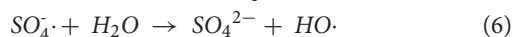
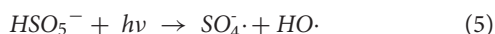


Ultraviolet Activation

Ultraviolet irradiation has been regarded as one of the most efficient approaches for PS/PMS activation because of the high irradiation energy of UV. The activation of PS/PMS under UV light is generally related to the cleavage of the O–O bond. Two $SO_4^{\cdot-}$ could be generated after the activation of PS (Equation 4), whereas $OH\cdot$ and $SO_4^{\cdot-}$ are generated through PMS activation because of its asymmetric structure (Equation 5). Similar to heat activation, some of the generated $SO_4^{\cdot-}$ could be further transformed to $OH\cdot$ through UV activation (Equation 6) (related



to the pH of the aqueous solution).



The work of Chen et al. (2019) found that $\text{SO}_4^{\cdot-}$ was the predominant radical under the condition of $\text{pH} < 7.0$, whereas $\text{SO}_4^{\cdot-}$ would convert to OH^- once the pH increased to 9.3 (Ao et al., 2018). Regarding different organic contaminants, UV/PS and UV/PMS have recently been employed for refractory organics degradation. Many studies have demonstrated that UV/PS shows a stronger oxidizing capacity for organic pollutants than UV/PMS, closely related to the higher quantum yielding (Carlson et al., 2015). However, UV merely accounts for a small fraction of solar light (3–5%); hence, the wavelength range for photoactivation of PS and PMS has recently been expanded from UV to visible light and even to solar light (Guo et al., 2018; Zhu et al., 2020).

Ultrasound Activation

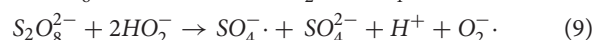
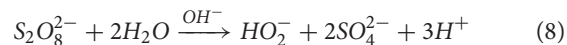
The main mechanisms of the ultrasonic activation of PS/PMS (related to cavitation bubbles) can be summarized as follows: (1) ultrasonic generation of sulfate radicals via homolysis of the O–O bond at high temperatures (5,000 K) and pressures (similar

to the energy-induced mechanism of heat and UV activation) (Matzek and Carter, 2016; Wang and Wang, 2018) and (2) generation of hydroxyl radicals and hydrogen radicals via the decomposition of water molecules under the action of cavitation bubbles (Equation 7). The recent work of Wang and Wang (2018) found that the yield of hydroxyl radicals was much higher than that of sulfate radicals under ultrasonic activation, especially for PS (Wang and Wang, 2018). However, the recombination rate of hydroxyl radicals was suppressed at high temperatures, owing to the low dissociation energy of the O–O bond of H_2O_2 . Thus, the concentration of hydroxyl radicals can reach the millimolar level under ultrasonic conditions (von Sonntag, 2008).



Where the symbol “~” represents ultrasonic range.

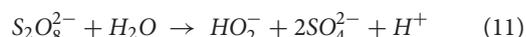
Tremendous works demonstrated that the ultrasound activation of PS was more suitable for sulfate radical generation at ambient temperature (Nasseri et al., 2017), and the increase in temperature would negatively affect its efficiency, especially when the temperature reached 65°C (Deng et al., 2015). Similar to heating activation, ultrasound still has the disadvantages of high cost and huge energy consumption. Moreover, ultrasound activation of PS can be easily achieved under alkaline conditions ($\text{pH} > 10$), and a tremendous amount of $\text{SO}_4^{\cdot-}$, superoxide ($\text{O}_2^{\cdot-}$), and OH^- is generated (Equations 8–10) (Nasseri et al., 2017).



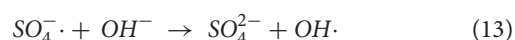
Chemical Activation Approaches

Alkaline Activation

Alkali activation of PS/PMS, one of the most widely used *in situ* approaches, involves increasing pH (usually $\text{pH} > 11$) via addition of sodium or potassium hydroxide (Matzek and Carter, 2016; Waclawek et al., 2017). Hydrolysis of one PS molecule to a hydrogen peroxide anion (HO_2^-) and, subsequently, to superoxide radicals ($\text{O}_2^{\cdot-}$) plays a key role in the activation process (Equations 11 and 12) (Matzek and Carter, 2016; Waclawek et al., 2017; Wang and Wang, 2018).

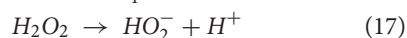
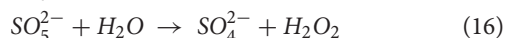
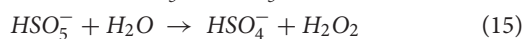
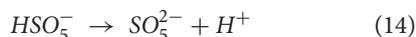


Moreover, sulfate radicals can further be converted to hydroxyl radicals under alkaline conditions (Equation 13) (Wang and Wang, 2018).

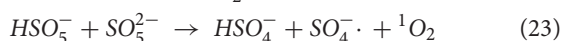
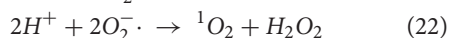
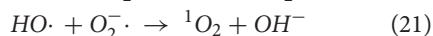
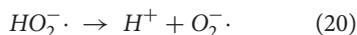
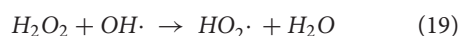


For PMS, alkaline activation exhibits quite a different pathway. As demonstrated by Qi et al. (2016), singlet oxygen and superoxide anion radicals are the predominant reactive oxygen species within the alkali/PMS system. Specifically, hydroxyl

radicals could be generated via the hydrolysis of HSO_5^- (Equations 14–18).



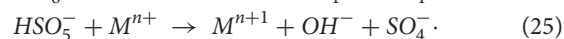
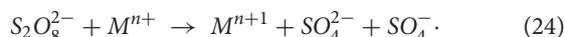
Subsequently, the abovementioned hydroxyl radical would further react with excessive hydrogen peroxide and generate superoxide anion radicals (Equations 19 and 20). The hydroxyl radical and superoxide anion radical would then be converted to singlet oxygen and hydroxide ions (Equation 21). In contrast, the superoxide anion radical can also generate hydrogen peroxide and singlet oxygen (Equation 22) (Qi et al., 2016). In addition, singlet oxygen can be generated via self-decomposition (Equation 23) (Wang and Wang, 2018).



Compared to that of heating, UV, and metal activations, the alkali-activated PS/PMS has the disadvantages of low efficiency and long degradation time (Crimi and Taylor, 2007; Huling et al., 2011). In addition, Zhao et al. (2013) found that the alkali-activated PS was not significant when used to degrade polycyclic aromatic hydrocarbons.

Transition Metal Ions and Metal Oxides

Besides the methods outlined above, PS and PMS can also be activated through transfer of an electron, using metals including cobalt, silver, manganese, and iron, for the formation of sulfate radicals (Equations 24 and 25 where M represents typical metal ions).

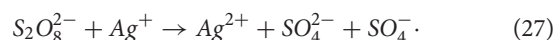


Yun et al. (2019) found that cobalt ions (Co^{2+}) could be applied as a catalyst for PMS activation for paracetamol degradation. Similarly, Ji et al. (2016a) showed that the generation of sulfate radicals within the Co(II)/PMS system could be applied to the degradation of tetrabromobisphenol A. The main reaction can be summarized as follows (Equation 26) (Hu and Long, 2016):

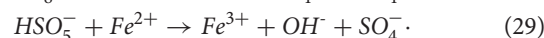


The main concern about using cobalt for PMS activation is its potential biological toxicity if used in substantial quantities. Thus,

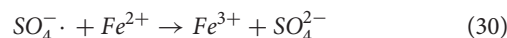
graphene, activated carbon, and metal oxides (Al_2O_3 , TiO_2 , MgO , etc.) have been widely applied to improve cobalt loading. Shi et al. (2012) proved that, compared with Co_3O_4 , the use of $\text{Co}_3\text{O}_4/\text{GO}$ for PMS activation significantly reduced cobalt leaching. For PS, silver ions are usually selected as one of the most efficient catalysts among the homogeneous metal ions and oxides (Zhou et al., 2018). Important research has demonstrated that the efficiency of PS activation is closely related to increased silver ion loading (Wang J. et al., 2017; Park et al., 2018; Ouyang et al., 2020) (Equation 27).



Fe ions and their oxides have also been widely studied, owing to their environmentally friendly, non-toxic, and low-cost characteristics (Wei et al., 2020). For example, Fe^{2+} -activated PS and PMS have been proven to be one of the most efficient pathways for sulfate radical generation (Equations 28 and 29) (Xiao et al., 2020).



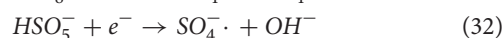
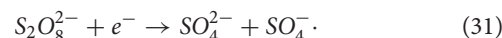
However, a large dose of Fe^{2+} results in a significant decline in the efficiency/scavenging ability of sulfate radicals (Equations 30) (Rastogi et al., 2009).



The use of metal ions in homogeneous systems for the activation of PS has the following limitations: (1) low recovery efficiency of metal ions; (2) restriction of reaction pH, with some of the metal ions always precipitating under basic conditions; and (3) organics within the systems negatively influencing the activation of PS and PMS. The abovementioned difficulties can partially be overcome in heterogeneous systems via a combination of metal ions with supports (such as metal oxide, molecular sieve, and carbonaceous material supports) (Xiao et al., 2020).

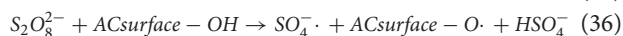
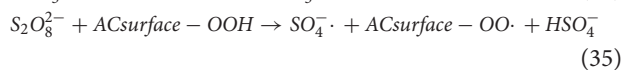
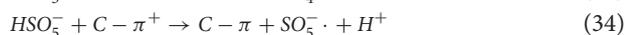
Carbon-Based Materials

Carbon-based materials, including activated carbon, graphene, carbon nanotubes, and biochar, have also recently been investigated for PS and PMS activation. The corresponding mechanisms of carbon-based materials in the formation of sulfate radicals, which usually act as an electron donor to PS or PMS, can be described by Equations (31)–(32):



In addition, the wide distribution of the catalytic moieties, such as quinone, carbonyl, and carboxyl groups, enhances the activation of PS and PMS via the formation of delocalized Π -electrons. The potential mechanism of PMS by carbon-based materials can be summarized in Equations (33)–(34). The corresponding

mechanisms of electron transfer from oxygen functional groups are shown in Equations (35)–(36).



Carbon nanotubes and graphene were recently applied to the activation of PS and PMS, to enhance efficiency. This is based on the textural structure and surface chemical properties of the carbon nanotubes and graphene during heteroatom doping. The recent work of Pan et al. (2018) found that the catalytic performance of carbonaceous materials improved significantly after nitrogen doping of the carbon nanotubes and graphite oxide. In addition, pyrolysis is widely applied to enhance the performance of carbon-based materials; for instance, the activation performance of biochar is significantly influenced by pyrolysis temperature and time (Zhao et al., 2017).

Coupling Activation Approaches

To further enhance the efficiency of activation using the abovementioned systems (heating, UV, alkaline and transition metal ions), hybrid activation systems have been promoted. For instance, cobalt-based catalysts (mentioned in the *Ultrasound Activation* section) exhibited a relatively high PMS activation performance; however, their poor thermal stability restricted their efficiency. Hence, combining cobalt-based catalysts with carbon materials, which provide more surface activation sites, has been widely applied (Bao et al., 2020). Recently, Amor et al. (2019) found that for winery wastewater treatment, the bulk removal efficiency of organics was much greater when using the heat/transition metal ions/S₂O₈²⁻ process, compared with the heat/S₂O₈²⁻ system. Similarly, ultrasound can induce heating/PS, thus enhancing their performance (Deng et al., 2015). Furthermore, Hu et al. (2020) inferred that microwave and Fe₃O₄ had a synergetic effect on PS activation (Hu et al., 2020).

Economic Analysis of Different Activation Methods for PS/PMS

Electricity/energy consumption (electricity consumed during the operation of the instruments and equipment) and reagent costs (such as catalytic and oxidation reagents) are the two main costs associated with PS/PMS activation processes. Theoretically, physical activation methods, such as heating, UV, and ultrasonic methods, are relatively economical compared with chemical activation, where the latter incur costs due to reagent consumption. However, physical activation approaches are less applicable in large-scale sewage treatment because of the high energy demand. Taking Fe(II)–PS/PMS systems as an example for organic compound removal from wastewater, only 0.47€ was needed per liter for Fe(II)-activated PS, whereas 4.40€ was needed for UV activation. Although carbon-based materials could be a promising activation method for PS/PMS, their high manufacturing cost restricts their use (even though most biochar is made from wood, sludge, and straw agricultural waste). Hybrid

activation always costs more than the other approaches, despite having a higher activation efficiency; thus, further research effort should focus on how to balance activation efficiency and cost.

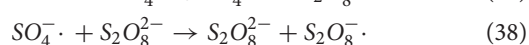
OXIDATION EFFICIENCY OF PS/PMS FOR CONTAMINANT DEGRADATION

Refractory contaminants such as pharmaceutical and personal care products (PPCPs), endocrine disruptors (EDCs), disinfection by-product precursors (DBPs), and high-concentration organic matter (HCOM) are abundant in aquatic environments; they seriously threaten human and ecosystem health. Sulfate-radical-based AOPs, which exhibit excellent efficiency in refractory organic pollutant removal, have recently been applied in the treatment of these contaminants. Because the PS/PMS oxidation systems have proven to be non-selective, degradation performance, efficiency, and possible intermediates are summarized here.

Performance of PS/PMS Oxidation

The degradation of antibiotics, DBPs, and EDCs within the PS/PMS system has been found to be hot spots requiring research attention, and their rate of degradation was recently used to efficiently evaluate their oxidation performance (Wang Q. et al., 2017; Amor et al., 2019; Qin et al., 2020a). **Table 2** shows that the degradation efficiency of the different pollutants is closely related to their chemical species/characteristics and the reaction conditions. Generally, the conditions such as temperature, pH, catalyst loading, and concentration of PS/PMS affect the removal rate of substances. For instance, the degradation efficiency of bisphenol A (BPA) was shown to increase gradually (in a linear relationship) from 46.7 to 66.4 to 76.8 to 96.4 and 99.0% with the PS concentrations increased from 7.4 to 15 to 22 to 30 and 35 mM (Xu et al., 2019). However, the degradation rate of ketoprofen (KET) increased from 69.4 to 97.3 to 100% when the pH gradually increased from 3 to 7 to 10, respectively (Feng et al., 2017).

On the other hand, the catalyst activity was shown to significantly influence the degradation of contaminants; this could be proven by the fact that the BPA degradation rate during PMS oxidation with a Sr₂CoFeO₆ catalyst was much higher than that for the reactors without a catalyst additive (Hammouda et al., 2018). The proportion of PS/PMS in the oxidation system was also essential to pollutant degradation because the excess quantity of PS can induce a reverse reaction, whereas the insufficient amount induces a low removal rate. The work of Li et al. (2019b) found that the increasing dosage of PS from 1 to 10 mmol/L accelerated the decolorization of reactive brilliant blue (RBB) from 50.42 to 93.75%; however, the excess PS consumed the generated SO₄⁻·, via the following reactions (detailed in Equations 37–38), and led to a significant declining of the overall removal rate of RBB.



Furthermore, the categories of substances also influenced the degradation rate. Under the same experimental conditions

TABLE 2 | Performance of typical pollutants under different reaction conditions.

	Pollutants	Reaction systems	Performances	References
PPCPs	Carbamazepine (CBZ)	LaCoO ₃ /PMS	<ul style="list-style-type: none"> LaCoO₃ calcinated at 600°C showed the best performance 91.8% of carbamazepine (100 mg/L) was removed within 30 min at pH 6–8 First-order kinetics 	Guo et al., 2020
	Levofloxacin hydrochloride (LVF)	CoFeO ₂ @CN/PMS	<ul style="list-style-type: none"> CoFeO₂@CN/PMS performed better than CoFeO₂@CN and PMS 89.4% of LVF (10 mg/L) was removed in 20 min using 0.2 g/L catalyst and 0.5 mM PMS 	Pi et al., 2020
	Ibuprofen (IBP)	N-doped graphene aerogel (NGA)/PMS	<ul style="list-style-type: none"> Catalytic activity increase exhibited NGA>NrGO>GA 100% of 20 mg/L IBP was removed in 60 min at 45°C Pseudo-first-order kinetics with activation energy of 87.5 kJ/mol 	Wang et al., 2019
	Sulfachloropyridazine (SCP)	Ni@NPC/PS	<ul style="list-style-type: none"> Catalytic activity of Ni@NPC>GO>N-rGO>MWCNTs 100% of SCP (>99%) was removed in 30 min at 45°C 	Kang et al., 2019
	Ketoprofen (KET)	Heat/PS	<ul style="list-style-type: none"> 100% of 10 μM KET was removed in 60 min at pH = 3 97.3% of 10 μM KET was removed in 60 min at pH = 7 69.4% of 10 μM KET was removed in 60 min at pH = 10 Pseudo-first-order kinetics with activation energy of 169.74 kJ/mol 	Feng et al., 2017b
	Caffeine (CAF)	Co-MCM41/PMS	<ul style="list-style-type: none"> Co-MCM41/PMS performed better than CoO/PMS or Co₃O₄/PMS 100% of 0.05 mM CAF was removed in 20 min using 200 mg/L catalyst and 0.2 mM PMS 	Qi et al., 2013
	Diclofenac (DCF)	BFO/PMS	<ul style="list-style-type: none"> 65.4% of 0.025 mM DCF was removed in 60 min at pH 3.0 using 0.5 mM PMS and 0.3 g/L BFO Following two separate concurrent pseudo-first-order catalytic process with different decay rates 	Han et al., 2020
	Sulfonamides (SAs)	Heat/PS	<ul style="list-style-type: none"> Conditions: reaction time 3 h, reaction temperature 60°C, 2 mM PS and 30 μM SAs, the removal rate of SMX, SIX, STZ, and SMT were 98, 100, 97, and 81%, respectively Pseudo-first-order kinetics with the activation energy of 109.8 ± 14.7, 133.9 ± 9.5, 130.8 ± 1.1, and 106.2 ± 3.5 kJ/mol for SMX, SIX, STZ, and SMT, respectively 	Zhou et al., 2019
	EDCs	Bisphenol A (BPA)	Magnetic CFA/PS	<ul style="list-style-type: none"> 76.9% of 0.22 mmol/L BPA was removed at 20°C and pH 5 in 60 min using 2 g/L magnetic CFA and 22 mM PS Pseudo-first-order kinetics 76.5% of 0.22 mmol/L BPA was removed at 20°C and pH 5 in 60 min using 2 g/L magnetic CFA and 22 mM PS Pseudo-first-order kinetics 70.2% of 0.22 mmol/L BPA was removed at 20°C and pH 5 in 60 min using 2 g/L magnetic CFA and 22 mM PS Pseudo-first-order kinetics
Bisphenol A (BPA)		CoS@GN-60/PMS	<ul style="list-style-type: none"> 92% of 20 mg/L BPA was removed at pH 6.65 in 8 min using 0.1 g/L catalysts and 0.1 g/L PMS First-order kinetics 	Zhu et al., 2019
Bisphenol F (BPF)		Sr ₂ FeCoO ₆ /PMS	<ul style="list-style-type: none"> Catalytic activity of Sr₂FeCoO₆ > SrCoO₃ > SrFeO₃ 100% of 20 mg/L BPF was removed at 55°C using 0.45 g/L Sr₂FeCoO₆ and 0.2 mM PMS Pseudo-first-order kinetics 	Hammouda et al., 2018
Tetrabromobisphenol A (TBBPA)		Co(II)/PMS	<ul style="list-style-type: none"> More than 96% of 9.2 μM TBBPA was removed at 20°C and pH 8.0 using 0.5 μM Co(II) and 0.2 mM PMS Pseudo-first-order kinetics 	Ji et al., 2016a
Iohexol		Co(II)/PMS	<ul style="list-style-type: none"> Almost 100% of 50 μM iohexol was removed in 30 min at 25°C and pH 7.0 using 4 mM PMS Pseudo-first-order kinetics 	Zhao et al., 2019
DBPs	Bromide	UV/PMS	<ul style="list-style-type: none"> 100% of bromide (initial concentration of 20 μM) was removal in 20 min at pH 7.0 and UV intensity 2.19 μE L⁻¹ s⁻¹ using ≥300 μM PS Follow pseudo-zero-order kinetics 	Fang and Shang, 2012
	Metolachlor (MET)	Co(II)/PMS	<ul style="list-style-type: none"> 100% of 10 mg/L MET was removed in 40 min at 25°C and pH 6.5 using 0.2 g/L CoFe₂O₄ and 3 mM PMS 	Liu C. et al., 2019
HCOMs	Clopyralid (CLP)	Heat/PS	<ul style="list-style-type: none"> The removal rate of CLP increased with increasing PS concentration 57 and 74% of CLP were removed at 50°C when the initial PS concentration was 1.0 and 2.0 mM, respectively 	Yang et al., 2020

(Continued)

TABLE 2 | Continued

Pollutants	Reaction systems	Performances	References
Landfill leachate	Heat/PS	<ul style="list-style-type: none"> • Acidic condition favored persulfate oxidation of leachate organics • High persulfate dose (PS:12COD₀) and high temperature enhanced the removal of COD and ammonia nitrogen • 100% of ammonia nitrogen was removed at 50°C and pH 5.3 when persulfate dose was 2 • 91% of COD was removed at 50°C and pH 4 when persulfate dose was 2 	Deng and Ezyske, 2011

(temperature and solution pH), the four typical antibiotics exhibited a decreasing trend—sulfisoxazole (100%) > sulfamethoxazole (98%) ≈ sulfathiazole (97%) > sulfamethizole (81%)—during the oxidation of PS/PMS (Zhou et al., 2019) (see Table 2).

Degradation Intermediates of Different Pollutants After PS/PMS Oxidation

Substitution, decarboxylation, destruction, coupling reaction, etc., accompanied by PS/PMS oxidation, have been shown to lead to distinct intermediate products during contaminant degradation. For instance, the oxidation of bisphenol F resulted in significant production of intermediates of bis(4-hydroxyphenyl)methanol, 4,4'-dihydroxybenzophenone, and 4-hydroxyphenyl 4-hydroxybenzoate as the PS/PMS oxidation progressed (Hammouda et al., 2018). The category of the intermediates is closely related to the degradation pathway and reaction conditions. Wu et al. (2020) found that the molecular weights of the oxidative intermediates of BPA within the Fe₂Co₁-LDH/PS system decreased significantly when the reaction time increased from 10 to 30 to 60 min. The addition of different catalytic components also significantly affects the intermediate products; for instance, the intermediates of BPA in the Fe₃O₄/coal fly ash/PS system were different from those obtained from the CoS@GN-60/PMS system (Zhu et al., 2019). In contrast, the intermediates of BPA in the BC-nZVI/PS system were phenol, p-hydroquinone, 4-isopropenylphenol, and 4-hydroxyacetophenone (Liu et al., 2018a); these are similar to those in the γ-Fe₂O₃@BC/PS system (Rong et al., 2019). Typical intermediates and their structural characteristics of the different containments during the PS/PMS oxidation are summarized in Table 3.

Experiments analyzing toxicity demonstrated that the majority of intermediates were less toxic than their parent pollutant. For example, the toxicity of the detectable intermediates of metolachlor (MET) (Liu C. et al., 2019), landfill leachate (Ghanbari et al., 2020), and carbamazepine (CBZ) (Guo et al., 2020) decreased significantly after PS/PMS oxidation. In contrast, the toxicity of intermediates produced from the degradation of highly concentrated organic wastewater increased significantly because of the formation of some halogenated organics (Wang Q. et al., 2017; Wang et al., 2020); the toxicity of the intermediates of alachlor was comparable to the formation of DBPs after chlorination within the ZVI/PS system (Wang et al., 2020). Similarly, Zhao et al. (2020) found

that the formation of chloronitrophenols during thermally activated PS oxidation increased the toxicity of the intermediates during the oxidation of 2-chlorophenol in the presence of nitrite (NO₂⁻) (see Table 3).

POTENTIAL DEGRADATION MECHANISMS OF PS/PMS OXIDATION

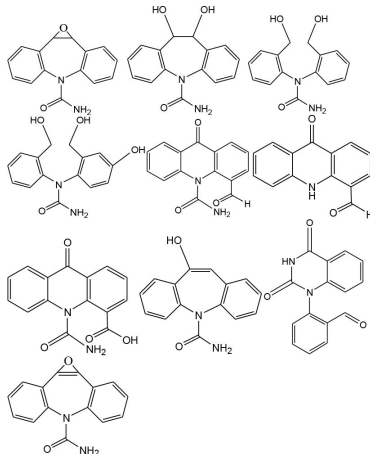
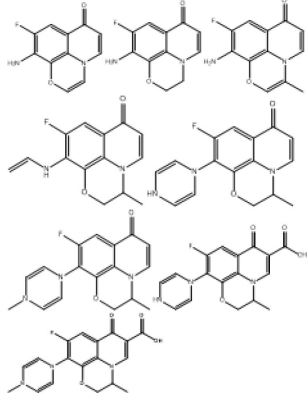
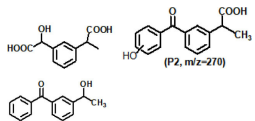
Sulfate and Other Radical Oxidation Mechanisms

Sulfate radicals are critical to the PS/PMS oxidation mechanism; in particular, the kinetic characteristics of the reaction are essential for improving oxidation efficiency. The sulfate radical plays a significant role in pollutant oxidation via the SR-AOP system (see Figure 2 for a summary of the potential mechanisms).

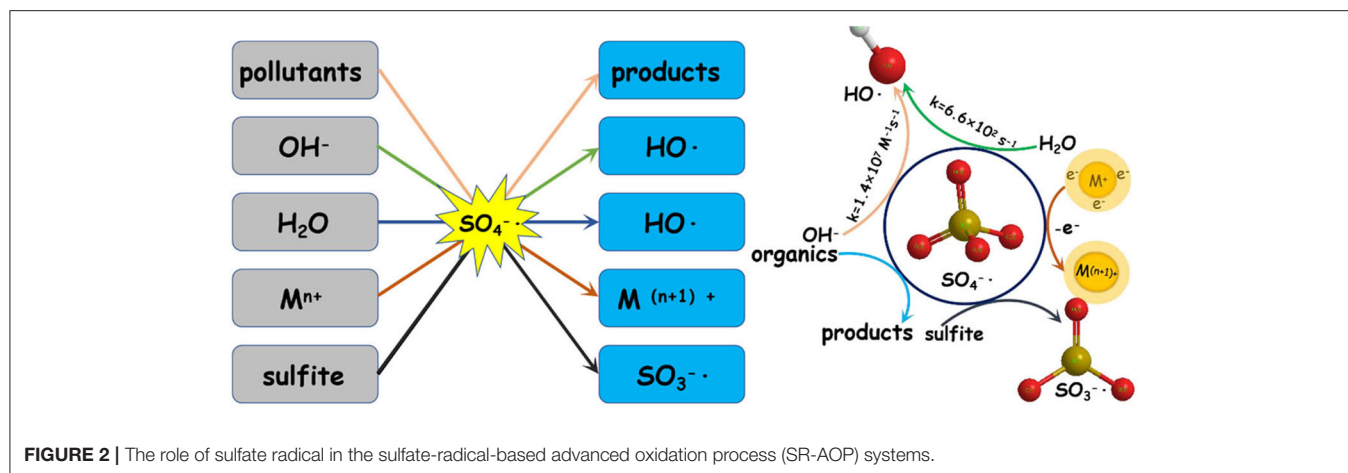
In the PS/PMS system, the degradation efficiency of SO₄^{-•} is closely related to the chemical properties of the substrates. For most free radical reactions, SO₄^{-•} is the primary reactive oxygen species, and its oxidation ability is 10⁴ times that of SO₅^{-•} (Zhou et al., 2018). Specifically, SO₄^{-•} can provide electrons to attack the unsaturated bond (–N=C–) of the target pollutant of caffeine (CAF), to form intermediates (Qi et al., 2013). However, the destruction of the benzene ring by SO₄^{-•} via hydrogen abstraction is the main pathway for BPA degradation (Zhao et al., 2016).

In addition to the organic substrates, the SO₄^{-•} generated can also react within aqueous solutions with sulfite and transition metal ions, as well as itself. Specifically, the most noteworthy sacrificial path of the generated SO₃^{-•} pool is the reaction between SO₄^{-•} and sulfite; the latter thus has a complicated role in SR-AOPs. Theoretically, increasing the sulfite concentration would improve the substrate oxidation efficiency. However, excessive sulfite will scavenge SO₄^{-•} and inhibit substrate oxidation. The concentration and behavior of SO₄^{-•} can be analyzed via radical trapping experiments and electron paramagnetic resonance detection (Liu Y. et al., 2019; Wu et al., 2020). Further oxidation of H₂O or OH⁻ by SO₄^{-•} leads to the generation of OH• (Equations 39–40), which would be another key reason for pollutant oxidation. The SO₄^{-•} and OH• produced can oxidize organic pollutants to different intermediates or inorganics through various degradation pathways (Hammouda et al., 2018). For example, Qi et al. (2013) found that the generated SO₄^{-•} and OH• radicals, with the Co²⁺/PMS system, can not only efficiently degrade caffeine but also mineralize the corresponding

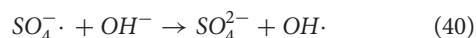
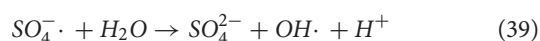
TABLE 3 | Chemical and structural characteristics of the intermediates of different pollutants during the PS/PMS oxidation.

Target pollutant	Catalytic system	Intermediates category and structure			References
		Open-chain compounds	Aromatic compounds	Heterocyclic compounds	
Carbamazepine	LaCoO ₃ /PMS				Guo et al., 2020
Levofloxacin hydrochloride (LVF)	CoFeO ₂ /CN/PMS				Pi et al., 2020
Ketoprofen (KET)	Heat/PS				Feng et al., 2017b

(Continued)



intermediates (see **Figure 2**).



The high concentration of sulfates, generated from the PS/PMS activation processes and side reactions, posed a potential threat to aquatic life (limited concentration of sulfate is 500 mg/L). However, the production and discharging of the sulfates during the PS/PMS activation are seldom focused. The recent studies revealed that one of the efficient approaches to overcome this limitation is the development of integrating the SR-AOP technique with cheaper oxidants, e.g., hydrogen peroxide or ozone (Duan et al., 2020). For example, Yang et al. (2015) proposed that the generated sulfates could be efficiently oxidated by the reaction of ozone with PMS.

Kinetic Characteristics of SR-AOPs Used in Organic Degradation

SR-AOPs are complicated physicochemical processes; studying the thermodynamic and kinetic characteristics of the reaction of different pollutants is essential for clarifying the mechanisms. Generally, the pseudo-first-order (Equation 39) and pseudo-second-order kinetics (Equation 40) have been widely used for the simulation of the degradation reaction of organic compounds; these can be described by linear forms in Equations (41) and (42), respectively.

$$\ln \frac{C_t}{C_0} = -k_1 t \quad (41)$$

$$\frac{1}{C_0} - \frac{1}{C_t} = -k_2 t \quad (42)$$

Where C_0 is the initial concentration of the pollutant, C_t represents the pollutant concentration at a certain reaction time (t), and k_1 and k_2 are the pseudo-first-order and pseudo-second-order rate constants, respectively.

The respective species and chemical structures of organic pollutants significantly affect the kinetic characteristics of

degradation. Some of the latest literature published revealing the kinetic mechanisms of typical organic pollutants during SR-AOPs is presented in **Table 4**. Overall, the degradation processes of (1) typical EDCs (such as bisphenol A, bisphenol F, and tetrabromobisphenol A) (Ji et al., 2016b; Hammouda et al., 2018; Xu et al., 2019) and (2) PPCPs (such as ketoprofen, ibuprofen, carbamazepine, etc.) (Feng et al., 2017; Wang et al., 2019; Guo et al., 2020) fit well with the pseudo-first-order kinetics. In contrast, the recent work of Lutze et al. (2015) found that the pseudo-second-order model yielded a much better fit for simulating the oxidation process of the chlorotriazine pesticides (such as atrazine, desethylterbuthylazine, and terbuthylazine).

It is interesting to note that the degradation of bisphenol S in a heat/PS system followed a pseudo-zero-order model (Wang Q. et al., 2017), whereas neither of the abovementioned zero-order, first-order, and pseudo-second-order models could be applied for the simulation of the degradation of diclofenac within the bismuth ferrite (BFO)/PMS system. Han et al. (2020) stated that the diclofenac degradation curve could be well-fitted to a double exponential expression, as shown in Equation (43).

$$\frac{C_t}{C_0} = a_1 e^{-k_1 t} + a_2 e^{-k_2 t} \quad (43)$$

Where C_t and C_0 are the diclofenac concentration (mM) at times t and 0, respectively; a_1 and a_2 represent fraction coefficients and k_1 and k_2 are the apparent rate constants (min^{-1}) for the first and second types of diclofenac degradation, respectively.

The reaction rates of different organic pollutants differ widely. Taking the reaction rate constant obtained from pseudo-first-order kinetics, for example, the abovementioned PPCPs, EDCs, and HCOM decrease in a trend of PPCPs (10^{-2} - 10^{-1}) \approx EDCs (10^{-2} - 10^{-1}) $>$ HCOM (10^{-4} - 10^{-3}). Specifically, the obtained k_1 value of ketoprofen was 0.26 min^{-1} in the heat/PS system at 70°C , whereas it declined to $3.29 \times 10^{-2} \text{ min}^{-1}$ when the temperature decreased to 60°C . The order of magnitude of the reaction rate constants was about 10^{-3} - 10^{-4} for pseudo-second-order kinetics (Khan et al., 2017). In addition, the changes in the experimental conditions could also affect the reaction rate constant; for example, the k_1 value of bisphenol

TABLE 4 | Kinetics model and rate constants of organic pollutants via SR-AOPs.

Pollutants	Kinetics	Rate constants	References
Ketoprofen	Pseudo-first-order	0.38 min ⁻¹	Feng et al., 2017
SCP	Pseudo-first-order	0.46 ± 2.3 × 10 ⁻³ min ⁻¹	Kang et al., 2019
Ibuprofen	Pseudo-first-order	0.0175 min ⁻¹	Wang et al., 2019
CBZ	Pseudo-first-order	0.26 min ⁻¹	Guo et al., 2020
Sulfonamides	Pseudo-first-order		Zhou et al., 2019
DEA	Pseudo-second-order	2.11 × 10 ⁻³ cm ² mJ ⁻¹	Khan et al., 2017
DIA	Pseudo-second-order	4.6 × 10 ⁻³ cm ² mJ ⁻¹	Khan et al., 2017
Clopyralid	Pseudo-first-order	3.29 × 10 ⁻² min ⁻¹	Yang et al., 2020
BPA	Pseudo-first-order	0.0556 min ⁻¹	Xu et al., 2020
BPS	Pseudo-first-order	0.0445 min ⁻¹	Liu Y. et al., 2019
BPF	Pseudo-first-order	0.026 min ⁻¹	Hammouda et al., 2018

A during the reaction significantly increased from 0.07 to 0.26 min⁻¹, when the catalyst loading increased from 0.2 to 0.4 g/L (Rong et al., 2019).

The species of radicals generated during SR-AOPs would also significantly affect the decomposition rate constant of the target pollutants. Zhao et al. (2016) reported that the degradation rate constant of BPA could be attributed to both the reactions with SO₄^{-•} and OH[•], respectively, which can be described by Equations (44).

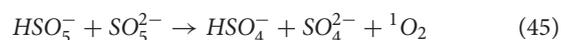
$$k_{obs} = k'_{SO_4^-} C_{SO_4^-} + k'_{OH} \cdot COH \quad (44)$$

Where k' represents the second-order rate constant for the reaction of BPA with each individual oxidizing species. Similarly, Wang et al. (2016) also found that the rate constants for the reaction of OH[•] were higher than those for SO₄^{-•} during the degradation process of 2,4-di-*tert*-butylphenol. Moreover, Nasser et al. (2017) found that the second-order rate constants of DEA [(6.42 ± 0.12) × 10⁸ M⁻¹ s⁻¹] and DIA [(1.70 ± 0.30) × 10⁹ M⁻¹ s⁻¹] under SO₄^{-•} oxidation were lower than those of OH[•]. [$k_{DEA} = (1.14 \pm 0.09) \times 10^9 \text{ M}^{-1} \text{ s}^{-1}$, $k_{DIA} = (2.22 \pm 0.44) \times 10^9 \text{ M}^{-1} \text{ s}^{-1}$] (see Table 4).

Possible Mechanism of SR-AOPs for Degradation of Different Organics

As the dominant radical, SO₄^{-•} oxidizes the pollutants primarily by the following mechanisms: (1) hydrogen abstraction, (2) electron transfer, and (3) addition or substitution reaction. Electron transfer is the predominant mechanism of the reaction between SO₄^{-•} and aromatic organics. Taking the SR-AOP degradation of, for example, ketoprofen (Feng et al., 2017), bisphenol F (Hammouda et al., 2018), and bisphenol A (Xu et al., 2019), the attack or destruction of the benzene ring by SO₄^{-•} might be the main reason for their degradation. By comparison, hydrogen abstraction could easily occur during SO₄^{-•} reaction with saturated organic compounds (e.g., alkanes, alcohols, organic acids, ethers, and esters) (Zhao et al., 2016). For alkene and alkyne organics, the single electrons of the sulfate radical would attack the unsaturated bonds, and addition or substitution would enhance the degradation.

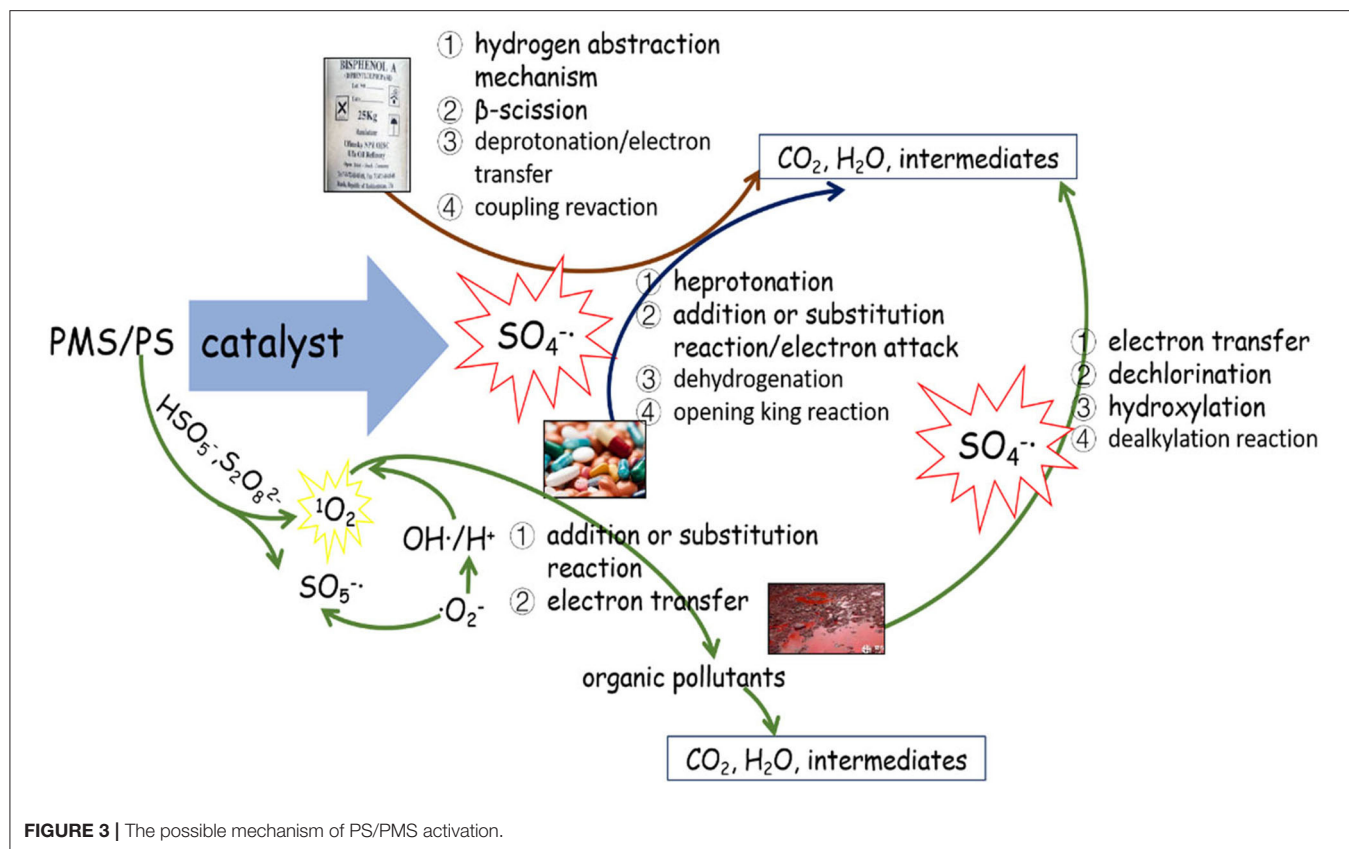
Generally, the concurrence of the abovementioned degradation pathways plays a significant role in the degradation of organic chemicals. For instance, the electrophilic attack of SO₄^{-•}, hydroxylation, and coupling reactions were the main reasons for BPA oxidation within the ZVI/PS system (Zhao et al., 2016). In contrast, a deprotonate radical attacking an unsaturated bond in oxidizing and substitution reactions belonged to the CAF during the application of the Co-MCM41/PMS system (Qi et al., 2013). The non-free radical reaction was another reason for the partial pollutant degradation. For instance, the ¹O₂ generated from the self-decomposition of PMS (via Equation 45) would attack pollutants/intermediates via an electron transfer mechanism. According to the recent work of Liu Y. et al. (2019), ¹O₂ could easily be generated either from the reactions between [•]O₂⁻ and OH[•]/H⁺ or from direct formation from SO₅^{-•} (see Figure 3).



SUMMARY AND OUTLOOK

Sulfate radicals can be effectively generated through PS or PMS activation by physical methods (such as heating, UV, and ultrasound) and chemical methods (including transition metal ions, alkaline conditions), as well as coupling activation methods. Overall, SR-AOPs can not only be applied to the treatment of refractory organics in wastewater but also are efficient in dealing with novel/emerging pollutants such as PPCPs, antibiotics, and DBP precursors. Not only can toxic pollutants be destroyed during SR-AOPs, but also the toxicity of most of the intermediates can also be reduced. Given the multiple sources of pollutants within wastewater and the complex reaction conditions, difficulty in implementing SR-AOPs for wastewater treatment is a barrier to PS/PMS oxidation. Therefore, we recommend the following research directions:

- (1) Prioritize research on the treatment/degradation of multiple pollutants using SR-AOP oxidation; in the municipal



wastewater treatment process, sewage is unlikely to contain only one target pollutant.

- (2) Develop novel and effective catalysts that can be used to upgrade the SR-AOP system to not only target pollutant directly but also efficiently improve the degradation efficiency of the pollutants.
- (3) Despite strong research proving that SR-AOPs are efficient at removing organic pollutants, dealing with wastewater at a large scale is still the main challenge. Therefore, a further direction is the search for alternative activation approaches that are economical and environment-friendly and can be applied in large-scale WWTPs.
- (4) Most researchers have focused on how to efficiently generate free radicals, but seldom on free radical or non-free radical degradation pathways for organics.

- (5) Research on the properties of intermediates, especially their toxicity, needs greater clarity. Thus, determining the fate of pollutants and their intermediates across their complete life cycle during SR-AOP oxidation should be prioritized.

AUTHOR CONTRIBUTIONS

All authors listed have made a substantial, direct and intellectual contribution to the work, and approved it for publication.

FUNDING

Funding was received from the National Nature Science Foundation of China (No. 51878213), the State Key Laboratory of Urban Water Resource and Environment (No. 2020TS01), and the Heilongjiang Nature Science Foundation (E2020093).

REFERENCES

- Amor, C., Rodríguez-Chueca, J., Fernandes, J. L., Domínguez, J. R., Lucas, M. S., and Peres, J. A. (2019). Winery wastewater treatment by sulphate radical based-advanced oxidation processes (SR-AOP): thermally vs. UV-assisted persulphate activation. *Proc. Saf. Environ. Protect.* 122, 94–101. doi: 10.1016/j.psep.2018.11.016
- Ao, X., Liu, W., Sun, W., Cai, M., Ye, Z., Yang, C., et al. (2018). Medium pressure UV-activated peroxymonosulfate for ciprofloxacin degradation: kinetics, mechanism, and genotoxicity. *Chem. E. J.* 345, 87–97. doi: 10.1016/j.cej.2018.03.133
- Babu, D. S., Srivastava, V., Nidheesh, P. V., and Kumar, M. S. (2019). Detoxification of water and wastewater by advanced oxidation processes. *Sci. Total Environ.* 696:133961. doi: 10.1016/j.scitotenv.2019.133961
- Bao, Y., Tian, M., Lua, S. K., Lim, T. T., Wang, R., and Hu, X. (2020). Spatial confinement of cobalt crystals in carbon nanofibers with oxygen vacancies as a high-efficiency catalyst for organics degradation. *Chemosphere* 245:125407. doi: 10.1016/j.chemosphere.2019.125407

- Cai, C., Zhang, H., Zhong, X., and Hou, L. W. (2015). Ultrasound enhanced heterogeneous activation of peroxymonosulfate by a bimetallic Fe–Co/SBA-15 catalyst for the degradation of Orange II in water. *J. Hazard Mater.* 283, 70–79. doi: 10.1016/j.jhazmat.2014.08.053
- Carlson, J. C., Stefan, M. I., Parnis, J. M., and Metcalfe, C. D. (2015). Direct UV photolysis of selected pharmaceuticals, personal care products and endocrine disruptors in aqueous solution. *Water Res.* 84, 350–361. doi: 10.1016/j.watres.2015.04.013
- Chen, Y., Li, M., Tong, Y., Liu, Z., Fang, L., Wu, Y., et al. (2019). Radical generation via sulfite activation on NiFe₂O₄ surface for estril removal: performance and mechanistic studies. *Chem. E. J.* 368, 495–503. doi: 10.1016/j.cej.2019.02.196
- Crimi, M. L., and Taylor, J. (2007). Experimental evaluation of catalyzed hydrogen peroxide and sodium persulfate for destruction of BTEX contaminants. *Soil Sediment Contaminat. Int. J.* 16, 29–45. doi: 10.1080/15320380601077792
- Deng, D., Lin, X., Ou, J., Wang, Z., Li, S., Deng, M., et al. (2015). Efficient chemical oxidation of high levels of soil-sorbed phenanthrene by ultrasound induced, thermally activated persulfate. *Chem. Eng. J.* 265, 176–183. doi: 10.1016/j.cej.2014.12.055
- Deng, Y., and Ezyske, C. M. (2011). Sulfate radical-advanced oxidation process (SR-AOP) for simultaneous removal of refractory organic contaminants and ammonia in landfill leachate. *Water Res.* 45, 6189–6194. doi: 10.1016/j.watres.2011.09.015
- Duan, X., Yang, S., Wacawek, S., Fang, G., Xiao, R., and Dionysiou, D. D. (2020). Limitations and prospects of sulfate-radical based advanced oxidation processes. *J. Environ. Chem. Eng.* 8:103849. doi: 10.1016/j.jece.2020.103849
- Fang, J. Y., and Shang, C. (2012). Bromate formation from bromide oxidation by the UV/persulfate process. *Environ. Sci. Tech.* 46, 8976–8983. doi: 10.1021/es300658u
- Feng, Y., Song, Q., Lv, W., and Liu, G. (2017). Degradation of ketoprofen by sulfate radical-based advanced oxidation processes: kinetics, mechanisms, and effects of natural water matrices. *Chemosphere* 189, 643–651. doi: 10.1016/j.chemosphere.2017.09.109
- Fernandes, A., Makóš, P., and Boczkaj, G. (2018). Treatment of bitumen post oxidative effluents by sulfate radicals based advanced oxidation processes (S-AOPs) under alkaline pH conditions. *J. Clean. Prod.* 195, 374–384. doi: 10.1016/j.jclepro.2018.05.207
- Ghanbari, F., Wu, J., Khatibasreh, M., and Lin, K. A. (2020). Efficient treatment for landfill leachate through sequential electrocoagulation, electrooxidation and PMS/UV/CuFe₂O₄ process. *Separat. Purif. Technol.* 242:116828. doi: 10.1016/j.seppur.2020.116828
- Guo, H., Zhou, X., Zhang, Y., Yao, Q., Qian, Y., Chu, H., et al. (2020). Carbamazepine degradation by heterogeneous activation of peroxymonosulfate with lanthanum cobaltite perovskite: performance, mechanism and toxicity. *J. Environ. Sci.* 91, 10–21. doi: 10.1016/j.jes.2020.01.003
- Guo, R., Xia, X., and Zhang, X. (2018). Construction of Ag₃PO₄/TiO₂ nano-tube arrays photoelectrode and its enhanced visible light driven photocatalytic decomposition of diclofenac. *Separat. Purif. Technol.* 200, 44–50. doi: 10.1016/j.seppur.2018.02.024
- Hammouda, S. B., Zhao, F., Safaei, Z., Ramasamy, D. L., Doshi, B., and Sillanpää, M. (2018). Sulfate radical-mediated degradation and mineralization of bisphenol F in neutral medium by the novel magnetic Sr₂CoFeO₆ double perovskite oxide catalyzed peroxymonosulfate: influence of co-existing chemicals and UV irradiation. *Appl. Catal. B Environ.* 233, 99–111. doi: 10.1016/j.apcatb.2018.03.088
- Han, F., Ye, X., Chen, Q., Long, H., and Rao, Y. (2020). The oxidative degradation of diclofenac using the activation of peroxymonosulfate by BiFeO₃ microspheres—kinetics, role of visible light and decay pathways. *Separat. Purif. Technol.* 232:115967. doi: 10.1016/j.seppur.2019.115967
- Hu, L., Wang, P., Zhang, G., Liu, G., Li, Y., Shen, T., et al. (2020). Enhanced persulfate oxidation of organic pollutants and removal of total organic carbons using natural magnetite and microwave irradiation. *Chem. Eng. J.* 383:123140. doi: 10.1016/j.cej.2019.123140
- Hu, P. D., and Long, M. C. (2016). Cobalt-catalyzed sulfate radical-based advanced oxidation: a review on heterogeneous catalysts and applications. *Appl. Catal. B Environ.* 181, 103–117. doi: 10.1016/j.apcatb.2015.07.024
- Huang, J., and Zhang, H. (2019). Mn-based catalysts for sulfate radical-based advanced oxidation processes: a review. *Environ. Int.* 133(Pt. A):105141. doi: 10.1016/j.envint.2019.105141
- Huling, S. G., Ko, S., Park, S., and Kan, E. (2011). Persulfate oxidation of MTBE- and chloroform-spent granular activated carbon. *J. Hazard Mater.* 192, 1484–1490. doi: 10.1016/j.jhazmat.2011.06.070
- Ji, Y., Kong, D., Lu, J., Jin, H., Kang, F., Yin, X., et al. (2016a). Cobalt catalyzed peroxymonosulfate oxidation of tetrabromobisphenol A: kinetics, reaction pathways, and formation of brominated by-products. *J. Hazard Mater.* 313, 229–237. doi: 10.1016/j.jhazmat.2016.04.033
- Ji, Y., Shi, Y., Dong, W., Wen, X., Jiang, M., and Lu, J. (2016b). Thermo-activated persulfate oxidation system for tetracycline antibiotics degradation in aqueous solution. *Chem. Eng. J.* 298, 225–233. doi: 10.1016/j.cej.2016.04.028
- Kang, J., Zhang, H., Duan, X., Tan, X., and Wang, S. (2019). Nickel in hierarchically structured nitrogen-doped graphene for robust and promoted degradation of antibiotics. *J. Clean. Prod.* 218, 202–211. doi: 10.1016/j.jclepro.2019.01.323
- Khan, J. A., He, X., Shah, N. S., Sayed, M., Khan, H. M., and Dionysiou, D. D. (2017). Degradation kinetics and mechanism of desethyl-atrazine and desisopropyl-atrazine in water with OH and SO₄ – based-AOPs. *Chem. Eng. J.* 325, 485–494. doi: 10.1016/j.cej.2017.05.011
- Li, H., Wan, J., Ma, Y., Wang, Y., Chen, X., and Guan, Z. (2016). Degradation of refractory dibutyl phthalate by peroxymonosulfate activated with novel catalysts cobalt metal-organic frameworks: mechanism, performance, and stability. *J. Hazard Mater.* 318, 154–163. doi: 10.1016/j.jhazmat.2016.06.058
- Li, J., Li, Y., Xiong, Z., Yao, G., and Lai, B. (2019a). The electrochemical advanced oxidation processes coupling of oxidants for organic pollutants degradation: a mini-review. *Chin. Chem. Lett.* 30, 2139–2146. doi: 10.1016/j.ccl.2019.04.057
- Li, W., Wu, P. X., Zhu, Y. J., Huang, Z. J., Lu, Y. H., Li, Y. W., et al. (2015). Catalytic degradation of bisphenol A by CoMnAl mixed metal oxides catalyzed peroxymonosulfate: performance and mechanism. *Chem. Eng. J.* 279, 93–102. doi: 10.1016/j.cej.2015.05.001
- Li, X., Tang, S., Yuan, D., Tang, J., Zhang, C., Li, N., et al. (2019b). Improved degradation of anthraquinone dye by electrochemical activation of PDS. *Ecotoxicol. Environ. Sci.* 177, 77–85. doi: 10.1016/j.ecoenv.2019.04.015
- Liu, C., Chen, L., Ding, D., and Cai, T. (2019). Sulfate radical induced catalytic degradation of metolachlor: efficiency and mechanism. *Chem. Eng. J.* 368, 606–617. doi: 10.1016/j.cej.2019.03.001
- Liu, C., Diao, Z., Huo, W., and Du, J. (2018a). Simultaneous removal of Cu²⁺ and bisphenol A by a novel biochar-supported zero valent iron from aqueous solution: synthesis, reactivity and mechanism. *Environ. Pollut.* 239, 698–705. doi: 10.1016/j.envpol.2018.04.084
- Liu, C., Wu, B., and Chen, X. (2018b). Sulfate radical-based oxidation for sludge treatment: a review. *Chem. Eng. J.* 335, 865–875. doi: 10.1016/j.cej.2017.10.162
- Liu, L., Gao, J., Liu, P., Duan, X., Han, N., Li, F., et al. (2019). Novel applications of perovskite oxide via catalytic peroxymonosulfate advanced oxidation in aqueous systems for trace L-cysteine detection. *J. Colloid Interface Sci.* 545, 311–316. doi: 10.1016/j.jcis.2019.03.045
- Liu, Y., Guo, H., Zhang, Y., Cheng, X., Zhou, P., Wang, J., et al. (2019). Fe@C carbonized resin for peroxymonosulfate activation and bisphenol S degradation. *Environ. Pollut.* 252, 1042–1050. doi: 10.1016/j.envpol.2019.05.157
- Lutze, H. V., Bircher, S., Rapp, I., Kerlin, N., Bakkour, R., Geisler, M., et al. (2015). Degradation of chlorotriazine pesticides by sulfate radicals and the influence of organic matter. *Environ. Sci. Tech.* 49, 1673–1680. doi: 10.1021/es503496u
- M'Arimi, M. M., Mecha, C. A., Kiprof, A. K., and Ramkat, R. (2020). Recent trends in applications of advanced oxidation processes (AOPs) in bioenergy production: review. *Renew. Sustain. Energy Rev.* 121:109669. doi: 10.1016/j.rser.2019.109669
- Martin-Diaz, J., Lucena, F., Blanch, A. R., and Jofre, J. (2020). Review: indicator bacteriophages in sludge, biosolids, sediments and soils. *Environ. Res.* 182:109133. doi: 10.1016/j.envres.2020.109133
- Matzek, L. W., and Carter, K. E. (2016). Activated persulfate for organic chemical degradation: a review. *Chemosphere* 151, 178–188. doi: 10.1016/j.chemosphere.2016.02.055
- Nasseri, S., Mahvi, A. H., Seyedsalehi, M., Yaghmaei, K., Nabizadeh, R., Alimohammadi, M., et al. (2017). Degradation kinetics of tetracycline in aqueous solutions using peroxydisulfate activated by ultrasound irradiation:

- effect of radical scavenger and water matrix. *J. Mol. Liquids* 241, 704–714. doi: 10.1016/j.molliq.2017.05.137
- Ouyang, M., Li, X., Xu, Q., Tao, Z., Yao, F., Huang, X., et al. (2020). Heterogeneous activation of persulfate by Ag doped BiFeO₃ composites for tetracycline degradation. *J. Colloid Interf. Sci.* 566, 33–45. doi: 10.1016/j.jcis.2020.01.012
- Pan, X., Chen, J., Wu, N., Qi, Y., Xu, X., Ge, J., et al. (2018). Degradation of aqueous 2,4,4'-Trihydroxybenzophenone by persulfate activated with nitrogen doped carbonaceous materials and the formation of dimer products. *Water Res.* 143, 176–187. doi: 10.1016/j.watres.2018.06.038
- Park, C., Heo, J., Wang, D., Su, C., and Yoon, Y. (2018). Heterogeneous activation of persulfate by reduced graphene oxide–elemental silver/magnetite nanohybrids for the oxidative degradation of pharmaceuticals and endocrine disrupting compounds in water. *Appl. Catal. B Environ.* 225, 91–99. doi: 10.1016/j.apcatb.2017.11.058
- Pi, Y., Gao, H., Cao, Y., Cao, R., Wang, Y., and Sun, J. (2020). Cobalt ferrite supported on carbon nitride matrix prepared using waste battery materials as a peroxymonosulfate activator for the degradation of levofloxacin hydrochloride. *Chem. Eng. J.* 379:122377. doi: 10.1016/j.cej.2019.122377
- Qi, C., Liu, X., Ma, J., Lin, C., Li, X., and Zhang, H. (2016). Activation of peroxymonosulfate by base: implications for the degradation of organic pollutants. *Chemosphere* 151, 280–288. doi: 10.1016/j.chemosphere.2016.02.089
- Qi, F., Chu, W., and Xu, B. (2013). Catalytic degradation of caffeine in aqueous solutions by cobalt-MCM41 activation of peroxymonosulfate. *Appl. Catal. B Environ.* 134–135, 324–332. doi: 10.1016/j.apcatb.2013.01.038
- Qin, K., Wei, L., Li, J., Lai, B., Zhu, F., Yu, H., et al. (2020b). A review of ARGs in WWTPs: Sources, stressors and elimination. *Chin. Chem. Lett.* 31, 2603–2613. doi: 10.1016/j.ccl.2020.04.057
- Qin, K. N., Chen, Y., Li, J. J., Xue, C. H., Wei, L. L., Song, X. G., et al. (2020a). Removal trends of sulfonamides and their ARGs during soil aquifer treatment and subsequent chlorination: effect of aerobic and anaerobic biodegradation. *Environ. Sci. Water Res. Technol.* 6:2331. doi: 10.1039/D0EW00270D
- Rastogi, A., Al-Abed, S. R., and Dionysiou, S. D. (2009). Sulfate radical-based ferrous–peroxymonosulfate oxidative system for PCBs degradation in aqueous and sediment systems. *Appl. Catal. B* 85, 171–179. doi: 10.1016/j.apcatb.2008.07.010
- Ren, W., Zhou, Z., Zhu, Y., Jiang, L., Wei, H., Niu, T., et al. (2015). Effect of sulfate radical oxidation on disintegration of waste activated sludge. *Int. Biodeter. Biodegr.* 104, 384–390. doi: 10.1016/j.ibiod.2015.07.008
- Rong, X., Xie, M., Kong, L., Natarajan, V., Ma, L., and Zhan, J. (2019). The magnetic biochar derived from banana peels as a persulfate activator for organic contaminants degradation. *Chem. Eng. J.* 372, 294–303. doi: 10.1016/j.cej.2019.04.135
- Seleiman, M. F., Santanen, A., and Mäkelä, P. S. A. (2020). Recycling sludge on cropland as fertilizer – advantages and risks. *Resour. Conserv. Recycl.* 155:104647. doi: 10.1016/j.resconrec.2019.104647
- Shi, P., Su, R., Wan, F., Zhu, M., Li, D., and Xu, S. (2012). Co₃O₄ nanocrystals on graphene oxide as a synergistic catalyst for degradation of Orange II in water by advanced oxidation technology based on sulfate radicals. *Appl. Catal. B Environ.* 123–124, 265–272. doi: 10.1016/j.apcatb.2012.04.043
- Song, H., Yan, L., Wang, Y., Jiang, J., Ma, J., Li, C., et al. (2019). Electrochemically activated PMS and PDS: radical oxidation versus nonradical oxidation. *Chem. Eng. J.* 391:123560. doi: 10.1016/j.cej.2019.123560
- Tsitonaki, A., Petri, B., Crimi, M., Mosbæk, H., Siegrist, R. L., and Bjerg, C. L. (2010). *In situ* chemical oxidation of contaminated soil and groundwater using persulfate: a review. *Crit. Rev. Environ. Sci. Tech.* 40, 55–91. doi: 10.1080/10643380802039303
- von Sonntag, C. (2008). Advanced oxidation processes: mechanistic aspects. *Water Sci. Technol.* 58, 1015–1021. doi: 10.2166/wst.2008.467
- Waclawek, S., Lutze, H. V., Grübel, K., Padil, V. V. T., and Cernik, M., Dionysiou, D. D. (2017). Chemistry of persulfates in water and wastewater treatment: a review. *Chem. Eng. J.* 330, 44–62. doi: 10.1016/j.cej.2017.07.132
- Wang, J., Ding, Y., and Tong, S. (2017). Fe–Ag/GAC catalytic persulfate to degrade Acid Red 73. *Separat. Purif. Technol.* 184, 365–373. doi: 10.1016/j.seppur.2017.05.005
- Wang, J., Duan, X., Dong, Q., Meng, F., Tan, X., Liu, S., et al. (2019). Facile synthesis of N-doped 3D graphene aerogel and its excellent performance in catalytic degradation of antibiotic contaminants in water. *Carbon* 144, 781–790. doi: 10.1016/j.carbon.2019.01.003
- Wang, J., and Wang, S. (2018). Activation of persulfate (PS) and peroxymonosulfate (PMS) and application for the degradation of emerging contaminants. *Chem. Eng. J.* 334, 1502–1517. doi: 10.1016/j.cej.2017.11.059
- Wang, Q., Lu, X., Cao, Y., Ma, J., Jiang, J., Bai, X., et al. (2017). Degradation of Bisphenol S by heat activated persulfate: kinetics study, transformation pathways and influences of co-existing chemicals. *Chem. Eng. J.* 328, 236–245. doi: 10.1016/j.cej.2017.07.041
- Wang, Q., Shao, Y., Gao, N., Liu, S., Dong, L., Rao, P., et al. (2020). Impact of zero valent iron/persulfate preoxidation on disinfection byproducts through chlorination of alachlor. *Chem. Eng. J.* 380:122435. doi: 10.1016/j.cej.2019.122435
- Wang, Q., Shen, X., Lu, X., Chen, J., and Zhu, Y. (2016). Degradation kinetics and mechanism of 2,4-Di-tert-butylphenol with UV/persulfate. *Chem. Eng. J.* 304, 201–208. doi: 10.1016/j.cej.2016.06.092
- Wei, L., Xia, X., Zhu, F., Li, Q., Xue, M., Li, J., et al. (2020). Dewatering efficiency of sewage sludge during Fe²⁺-activated persulfate oxidation: effect of hydrophobic/hydrophilic properties of sludge EPS. *Water Res.* 181:115903. doi: 10.1016/j.watres.2020.115903
- Wu, L., Hong, J., Zhang, Q., Chen, B. Y., Wang, J., and Dong, Z. (2020). Deciphering highly resistant characteristics to different pHs of oxygen vacancy-rich Fe₂Co₁-LDH/PS system for bisphenol A degradation. *Chem. Eng. J.* 385:123620. doi: 10.1016/j.cej.2019.123620
- Xiao, R., Luo, Z., Wei, Z., Luo, S., Spinney, R., Yang, W., et al. (2018). Activation of peroxymonosulfate/persulfate by nanomaterials for sulfate radical-based advanced oxidation technologies. *Curr. Opin. Chem. Eng.* 19, 51–58. doi: 10.1016/j.coche.2017.12.005
- Xiao, S., Cheng, M., Zhong, H., Liu, Z., Liu, Y., Yang, X., et al. (2020). Iron-mediated activation of persulfate and peroxymonosulfate in both homogeneous and heterogeneous ways: a review. *Chem. E. J.* 384:123265. doi: 10.1016/j.cej.2019.123265
- Xu, L., Fu, B., Sun, Y., Jin, P., Bai, X., Jin, X., et al. (2020). Degradation of organic pollutants by Fe/N co-doped biochar via peroxymonosulfate activation: Synthesis, performance, mechanism and its potential for practical application. *Chem. E. J.* 400:125870. doi: 10.1016/j.cej.2020.125870
- Xu, X., Zong, S., Chen, W., and Liu, D. (2019). Comparative study of Bisphenol A degradation via heterogeneously catalyzed H₂O₂ and persulfate: reactivity, products, stability and mechanism. *Chem. Eng. J.* 369, 470–479. doi: 10.1016/j.cej.2019.03.099
- Yang, Q., Ma, Y., Chen, F., Yao, F., Sun, J., Wang, S., et al. (2019). Recent advances in photo-activated sulfate radical-advanced oxidation process (SR-AOP) for refractory organic pollutants removal in water. *Chem. Eng. J.* 378:122149. doi: 10.1016/j.cej.2019.122149
- Yang, S., Wang, P., Yang, X., Shan, L., Zhang, W., Shao, X., et al. (2010). Degradation efficiencies of azo dye Acid Orange 7 by the interaction of heat, UV and anions with common oxidants: persulfate, peroxymonosulfate and hydrogen peroxide. *J. Hazard. Mater.* 179, 552–558. doi: 10.1016/j.jhazmat.2010.03.039
- Yang, W., Jiang, Z., Hu, X., Li, X., Wang, H., and Xiao, R. (2019). Enhanced activation of persulfate by nitric acid/annealing modified multi-walled carbon nanotubes via non-radical process. *Chemosphere* 220, 514–522. doi: 10.1016/j.chemosphere.2018.12.136
- Yang, X., Ding, X., Zhou, L., Fan, H. H., Wang, X., Ferronato, C., et al. (2020). New insights into clopyralid degradation by sulfate radical: pyridine ring cleavage pathways. *Water Res.* 171:115378. doi: 10.1016/j.watres.2019.115378
- Yang, Y., Jiang, J., Lu, X., Ma, J., and Liu, Y. (2015). Production of sulfate radical and hydroxyl radical by reaction of ozone with peroxymonosulfate: a novel advanced oxidation process. *Environ. Sci. Technol.* 49, 7330–7339. doi: 10.1021/es506362e
- Yun, W. C., Lin, K. Y. A., Tong, W. C., Lin, Y. F., and Du, Y. (2019). Enhanced degradation of paracetamol in water using sulfate radical-based advanced oxidation processes catalyzed by 3-dimensional Co₃O₄ nanoflower. *CEJ*, 373, 1329–1337. doi: 10.1016/j.cej.2019.05.142
- Zhao, D., Liao, X., Yan, X., Huling, S. G., Chai, T., and Tao, H. (2013). Effect and mechanism of persulfate activated by different methods for PAHs removal in soil. *J. Hazard. Mater.* 254–255, 228–235. doi: 10.1016/j.jhazmat.2013.03.056

- Zhao, H., Ji, Y., Kong, D., Lu, J., Yin, X., and Zhou, Q. (2019). Degradation of iohexol by Co^{2+} activated peroxymonosulfate oxidation: Kinetics, reaction pathways, and formation of iodinated byproducts. *Chem. Eng. J.* 373, 1348–1356. doi: 10.1016/j.cej.2019.05.140
- Zhao, L., Ji, Y., Kong, D., Lu, J., Zhou, Q., and Yin, X. (2016). Simultaneous removal of bisphenol A and phosphate in zero-valent iron activated persulfate oxidation process. *Chem. Eng. J.* 303, 458–466. doi: 10.1016/j.cej.2016.06.016
- Zhao, Q., Mao, Q., Zhou, Y., Wei, J., Liu, X., Yang, J., et al. (2017). Metal-free carbon materials-catalyzed sulfate radical-based advanced oxidation processes: a review on heterogeneous catalysts and applications. *Chemosphere* 189, 224–238. doi: 10.1016/j.chemosphere.2017.09.042
- Zhao, X., Zhang, T., Lu, J., Zhou, L., Chovelon, J.-M., and Ji, Y. (2020). Formation of chloronitrophenols upon sulfate radical-based oxidation of 2-chlorophenol in the presence of nitrite. *Environ. Pollut.* 261:114242. doi: 10.1016/j.envpol.2020.114242
- Zhou, D., Chen, L., Li, J., and Wu, F. (2018). Transition metal catalyzed sulfite auto-oxidation systems for oxidative decontamination in waters: a state-of-the-art minireview. *Chem. E. J.* 346, 726–738. doi: 10.1016/j.cej.2018.04.016
- Zhou, L., Yang, X., Ji, Y., and Wei, J. (2019). Sulfate radical-based oxidation of the antibiotics sulfamethoxazole, sulfisoxazole, sulfathiazole, and sulfamethizole: the role of five-membered heterocyclic rings. *Sci. Total Environ.* 692, 201–208. doi: 10.1016/j.scitotenv.2019.07.259
- Zhu, C., Liu, F., Ling, C., Jiang, H., Wu, H., and Li, A. (2019). Growth of graphene-supported hollow cobalt sulfide nanocrystals via MOF-templated ligand exchange as surface-bound radical sinks for highly efficient bisphenol A degradation. *Appl. Catal. B Environ.* 242, 238–248. doi: 10.1016/j.apcatb.2018.09.088
- Zhu, F. Y., Lv, Y. Z., Li, J. J., Ding, J., Xia, X. H., Wei, L. L., et al. (2020). Enhanced visible light photocatalytic performance with metal-doped Bi_2WO_6 for typical fluoroquinolones degradation: efficiencies, pathways and mechanisms. *Chemosphere* 252:126577. doi: 10.1016/j.chemosphere.2020.126577

Conflict of Interest: The authors declare that the research was conducted in the absence of any commercial or financial relationships that could be construed as a potential conflict of interest.

Copyright © 2020 Xia, Zhu, Li, Yang, Wei, Li, Jiang, Zhang and Zhao. This is an open-access article distributed under the terms of the Creative Commons Attribution License (CC BY). The use, distribution or reproduction in other forums is permitted, provided the original author(s) and the copyright owner(s) are credited and that the original publication in this journal is cited, in accordance with accepted academic practice. No use, distribution or reproduction is permitted which does not comply with these terms.